Supplementary Material - NC-PDNet: Density-Compensated Unrolled Networks for 2D and 3D non-Cartesian MRI Reconstruction

Zaccharie Ramzi, Chaithya G R, Jean-Luc Starck and Philippe Ciuciu *Senior Member, IEEE*

S1. Formal definition of the NDFT

Let us give the mathematical definition of $\hat{\boldsymbol{f}}$, the d dimensional discrete NDFT of a signal $\boldsymbol{f}$, for sample locations $(\boldsymbol{r}_i \in [-\frac{1}{2}; \frac{1}{2})^d)_{i=0\dots M}$ and frequency indices $(\boldsymbol{k}_j)_{j=0\dots K}$:

$$\boldsymbol{f}_i = \sum_{j=0}^{K} \hat{\boldsymbol{f}}_j \exp(-2i\pi \boldsymbol{k}_j^T \boldsymbol{r}_i) \tag{S1}$$

You can find more details about this in [1].

S2. Density compensation bias correction

If we simply apply the density compensation to recover the naive reconstruction of the k-space, $\mathbb{S}^H \mathcal{F}_\Omega^H \boldsymbol{d}_N \mathcal{Y}$, the obtained image has a scalar multiplicative bias. We correct this bias in the density compensation weights by simply computing it for an image with values 1 and dividing the density compensation weights by this bias b_d:

$$b_d = \mathcal{F}_\Omega^H \boldsymbol{d}_N \mathcal{F}_\Omega \mathbf{1} \tag{S2}$$

S3. 3D Trajectories

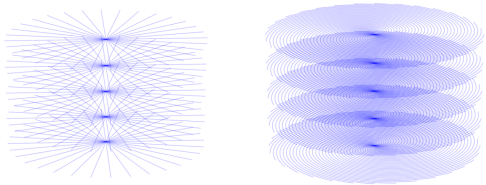

Radial **Spiral**

Fig. S1: Schematical illustration of the 2 k-space trajectories considered in this work for 3D imaging. Each of them uses 100 spokes and has a total of 64k measurements stacked 176 times across the additional dimension (here only 5 stacks are represented).

S4. Training details

The training is done with a compound ℓ_1 - Multi-scale SSIM [2] loss as advised by the winners of the 2019 fastMRI challenge [3]. We used the Rectified Adam optimizer [4] with default parameters from the TensorFlow implementation[1] and a learning rate of 10^{-4}. We used a batch size of 1, in order for the models to fit on a single V100 GPU with 32GB of memory. For the 2D settings, we used 100 epochs for training (97.3k gradient steps), where an epoch is defined as seeing one slice of each volume in the dataset. For the 3D setting we used 8 epochs for training (∼26k gradient steps). For the fastMRI data, the k-space is scaled up by a factor of 10^6 as per [5]. We scaled the OASIS data by a factor of 10^{-2}. The training times for the different networks in the different settings can be found in Tab. I.

[1] `tensorflow.org/addons/api_docs/python/tfa/optimizers/RectifiedAdam`

TABLE I: Training times in hours (h) for the different networks in the different settings.

Model	Single-coil 2D	Multi-coil 2D	Single-coil 3D
U-net on Adjoint + DC	8 h	20 h	22 h
NC-PDNet	24 h	34 h	196 h

S5. Additional qualitative results

In Fig. S2, for the spiral acquisition, as was hinted by the quantitative results in Tab. I in the main text, we can see that the difference between the *NC-PDNet* and U-net with DC is harder to grasp.

In Fig. S3, we can see that for the spiral acquisition, there is virtually no difference between the U-net and *NC-PDNet*'s results. We could say that the error map is slightly flatter in the *NC-PDNet* case.

The Fig. S4 illustrates the reconstructions obtained for the 3D setting with a stack of radial acquisition.

We advise the reader that, in the case of the spiral acquisition in Fig. S5, the non-flatness in the error map comes from areas outside of the organ and are due to artifacts in the ground truth.

References

[1] J. Keiner, S. Kunis, and D. Potts, "Using NFFT 3 - -A software library for various nonequispaced fast fourier transforms," *ACM Transactions on Mathematical Software*, vol. 36, no. 4, pp. 1–30, 2009.

[2] Z. Wang, E. Simoncelli, and A. C. Bovik, "Multi-Scale Structural Similarity for Image Quality Assessment," *Proceedings of the 37th IEEE Asilomar Conference on Signals, Systems and Computers*, vol. 2, pp. 9–13, 2003.

[3] N. Pezzotti, S. Yousefi, M. S. Elmahdy, J. Van Gemert, C. Schülke, M. Doneva, T. Nielsen, S. Kastryulin, B. P. F. Lelieveldt, M. J. P. Van Osch, E. De Weerdt, and M. Staring, "An Adaptive Intelligence Algorithm for Undersampled Knee MRI Reconstruction: Application to the 2019 fastMRI Challenge," Tech. Rep., 2019. [Online]. Available: https://arxiv.org/abs/2004.07339

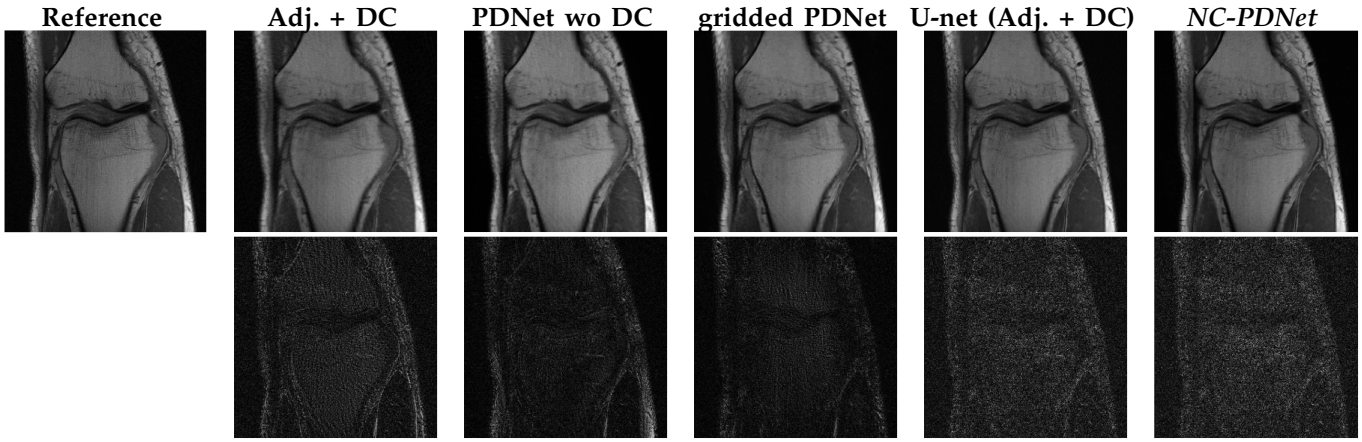

Fig. S2: **2D single-coil spiral acquisition (knee fast MRI dataset)**: Reconstruction results for a specific slice (16th slice of `file1001184`, part of the validation set). The top row represents the reconstruction using the different methods, while the bottom one represents the absolute error when compared with the reference.

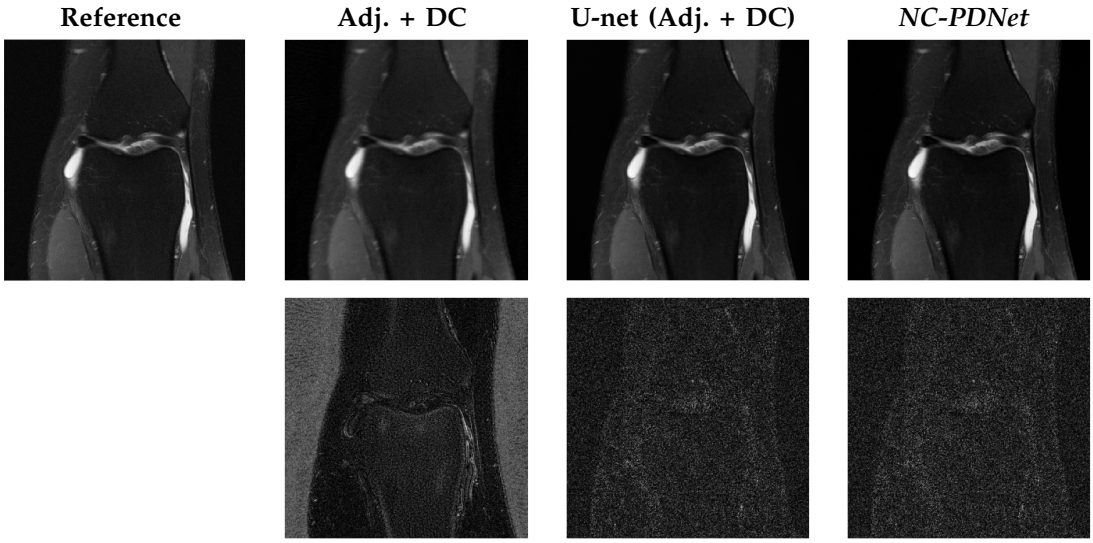

Fig. S3: **2D multi-coil spiral acquisition (knee fast MRI dataset)**: Reconstruction results for a specific slice (16th slice of `file1000000`, part of the validation set). The top row represents the reconstruction using the different methods, while the bottom one represents the absolute error when compared with the reference.

[4] L. Liu, H. Jiang, P. He, W. Chen, X. Liu, J. Gao, and J. Han, "On the Variance of the Adaptive Learning Rate and Beyond," in *Proceedings of International Conference for Learning Representations*, 2020.

[5] Z. Ramzi, P. Ciuciu, and J. L. Starck, "Benchmarking MRI reconstruction neural networks on large public datasets," *Applied Sciences (Switzerland)*, vol. 10, no. 5, 2020.

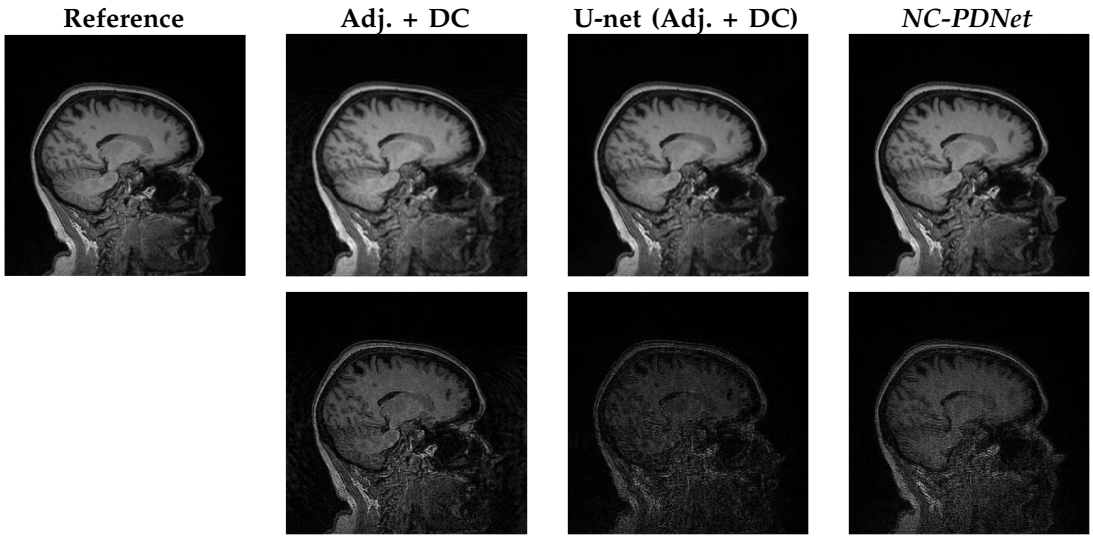

Fig. S4: **3D stack-of-stars acquisition (OASIS dataset, T1 contrast)**: Reconstruction results for a specific slice (101st slice of `sub-OAS30001_ses-d0129_run-01_T1w`, part of the validation set). The top row represents the reconstruction using the different methods, while the bottom one represents the absolute error when compared with the reference.

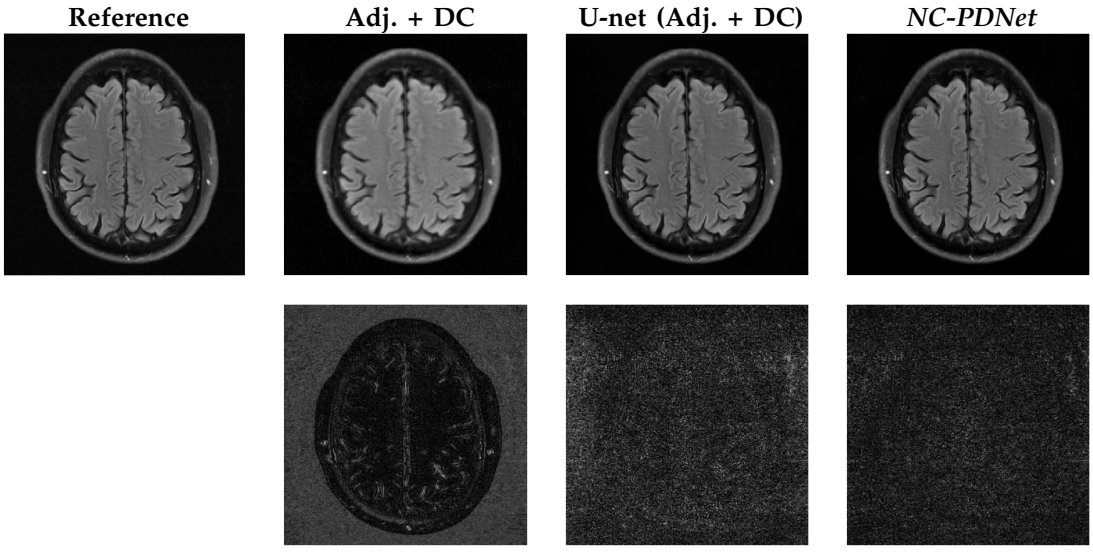

Fig. S5: **2D multi-coil spiral acquisition**: Reconstruction results for a specific slice (6th slice of `file_brain_AXFLAIR_200_6002447`) from the brain fastMRI dataset with networks trained on knee data. The top row represents the reconstruction using the different methods, while the bottom one represents the absolute error when compared with the reference.